

**Photogeneration Dynamics  
of  
a Soliton Pair in Polyacetylene**

Yukio HIRANO\* and Yoshiyuki ONO\*\*

*Department of Physics, Toho University, Miyama 2-2-1, Funabashi, Chiba 274-8510*

(Received 15 June 1998)

Dynamical process of the formation of a soliton pair from a photogenerated electron-hole pair in polyacetylene is studied numerically by adopting the SSH Hamiltonian. A weak local disorder is introduced in order to trigger the formation. Starting from an initial configuration with an electron at the bottom of the conduction band and a hole at the top of the valence band, separated by the Peierls gap, the time dependent Schrödinger equation for the electron wave functions and the equation of motion for the lattice displacements are solved numerically. After several uniform oscillations of the lattice system at the early stage, a large distortion corresponding to a pair of a soliton and an anti-soliton develops from a point which is determined by the location and type of the disorder. In some cases, two solitons run in opposite directions, leaving breather like oscillations behind, and in other cases they form a bound state emitting acoustic lattice vibrational modes.

KEYWORDS: polyacetylene, charged soliton, neutral soliton, bond-type disorder, site-type disorder, breather, simulation of soliton dynamics, soliton confinement, photogeneration of soliton

## §1. Introduction

Polyacetylene is the simplest conjugated polymer. There are many physically interesting phenomena in the polyacetylene, such as unusual optical and electronic properties which are not seen in other organic polymers. Those phenomena have been found in the experimental and theoretical studies during the last two decades. It was predicted<sup>1)</sup> that a photogenerated electron-hole pair would decay within a few picoseconds<sup>2,3)</sup> into a pair of solitons. This theoretical prediction has excited a lot of studies on transient spectroscopy of polymers. It has been pointed out that there exist the soliton and the polaron as typical elementary excitations in the *trans*-polyacetylene.<sup>4,5)</sup> Infrared and Raman activities of polyacetylene have also been studied intensively and vibrational

---

\* E-mail : hirano@ph.sci.toho-u.ac.jp

\*\* E-mail : ono@polaron.ph.sci.toho-u.ac.jp

modes induced by the existence of solitons have been confirmed.<sup>6-9)</sup> The soliton in polyacetylene is a complex nonlinear excitation created by the coupling between the electronic and the lattice degrees of freedom. There are two kinds of soliton, a charged soliton and a neutral soliton.<sup>3,10)</sup> The charged soliton has a unit charge, and its spin is zero. As for the neutral soliton, it has a spin of magnitude 1/2 but no charge. It has also been confirmed with the computer simulations by A.R.Bishop and coworkers<sup>11,12)</sup> that under a certain condition there exists a localized excitation called a breather which oscillates with a certain frequency.

So far many efforts have been devoted to numerical studies of dynamical behaviors of solitons and related nonlinear excitations in polyacetylene.<sup>13-18)</sup> Most studies have focused on the energy difference between different static configurations of solitons, polarons or bipolarons. However the dynamical process of the photoexcitation of solitons has not yet been studied intensively. Phillipot et al.<sup>12)</sup> carried out dynamical simulations on the photo-induced formation of nonlinear excitations. In their work, the dynamics of the electron system is treated within so-called “adiabatic dynamics”; namely the electronic configurations are determined for eigenstates of the instantaneous Hamiltonian at each time. If the lattice relaxation process is discussed within this treatment, the total energy is not conserved as is well-known.<sup>15)</sup> In the present work we report the results of numerical simulations for the formation process of a soliton-antisoliton pair from a photoexcited electron-hole pair in the perfectly dimerized background. The electronic configurations are determined for the eigenstates of the initial Hamiltonian as done in the series of numerical works on the soliton dynamics in an electric field.<sup>15-18)</sup> In this treatment the total energy is conserved. Although the importance of the mutual Coulomb interaction among electrons is pointed out, we use the standard Su-Schrieffer-Heeger (SSH) model without the Coulomb interactions. This is partly because of simplicity and partly because we want to concentrate ourselves to the formation process of a soliton-antisoliton pair. In the presence of the Coulomb interaction, the possibility of an exciton formation cannot be excluded. The effect of the electron-electron interaction will be treated in the future studies.

The optical excitation process of solitons can be decomposed into two steps. The first step is the creation of an electron-hole pair by photoabsorption. The second step is the decay process of this electron-hole pair into a soliton pair. The latter step involves the lattice relaxation, and therefore is much slower than the former which is a purely electronic process. We discuss only the latter in this paper. In principle there might be a coherence between the two steps.<sup>19)</sup> We assume, however, that the coherence can be neglected because of the large difference in the characteristic time scale. The radiative recombination process of the electron-hole pair is also excluded from the consideration.

The paper is organized as follows. In the next section the model and the method of simulation is explained. The results of simulations are described in §3. The last section is devoted to concluding remarks.

## §2. Model and Method of Simulation

The procedure of simulation is summarized as follows. At first, we solve a static problem where the system is in the ground state with a perfectly dimerized chain and with electronic levels just half-filled. Thus, the half of the electronic states are occupied by the up and down spin electrons. As the next step we create artificially an electron-hole pair by moving one electron from the top of the valence band to the bottom of the conduction band across the Peierls gap, in order to mimic the photo-excitation. The details of this excitation process are disregarded, since the actual optical excitation process is considered to occur within a very short time. We take this excited state with an electron-hole pair as the initial state of the dynamical simulation and pursue the time dependence of the lattice displacements and the electronic wave functions.

In this paper we employ the SSH model which is considered to be a standard model for *trans*-polyacetylene.

$$H = - \sum_{n,s} [t_0 - \alpha(u_{n+1} - u_n)](c_{n+1,s}^\dagger c_{n,s} + c_{n,s}^\dagger c_{n+1,s}) + \sum_n \frac{K}{2}(u_{n+1} - u_n)^2 + \sum_n \frac{M}{2}\dot{u}_n^2 + H', \quad (1)$$

where  $t_0$  is the transfer integral between the nearest neighbor sites in the equidistant lattice,  $\alpha$  the electron phonon coupling. The second and third terms of eq. (1) represent the lattice potential energy mainly due to  $\sigma$ -bonding and the kinetic energy of CH-units, respectively:  $u_n$  the displacement of the  $n$ -th CH-unit,  $K$  the spring constant and  $M$  the mass of a CH-unit. The last term describes the part related to disorders and expressed as

$$H' = V_s \sum_{i,s} c_{i,s}^\dagger c_{i,s}, \quad (2)$$

in the case of site-type disorders, and as

$$H' = -V_b \sum_{i,s} (c_{i,s}^\dagger c_{i+1,s} + c_{i+1,s}^\dagger c_{i,s}), \quad (3)$$

in the case of bond-type disorders.<sup>20)</sup> Here  $i$  denotes the position of a disorder.

The number of lattice points,  $N$ , is chosen as a multiple of four, in order to have a perfectly dimerized ground state with a non-degenerate top state of the valence band and with a non-degenerate bottom state of the conduction band. The total number of electrons is set to be equal to  $N$  so that the half-filled ground state may be realized. As described above, we prepare first the ground state which should be fully self-consistent with respect to both degrees of freedom of the electrons and lattice displacements. The ground state is obtained by iteration as in previous works.<sup>15-18)</sup> The iteration is repeated until the ratio between the two sums,  $\sum_n (y_n^{(i+1)} - y_n^{(i)})^2$  and  $\sum_n (y_n^{(i+1)})^2$ , becomes less than  $10^{-15}$ , where  $y_n^{(i)}$  indicates the value of  $y_n$  at the  $i$ -th iteration.

After having obtained the perfectly dimerized ground state we change the occupation numbers of the valence band top state and the conduction band bottom state so as to get the initial state with an electron-hole pair. The equation of motion for the bond variable  $y_n (\equiv u_{n+1} - u_n)$  is expressed in the form,

$$M\ddot{y}_n = F(t), \quad (4)$$

where

$$\begin{aligned} F(t) = & K(y_{n+1} - 2y_n + y_{n-1}) \\ & + 2\alpha \text{Re} [(B_{n+1,n+2} - 2B_{n,n+1} + B_{n-1,n})], \end{aligned} \quad (5)$$

with

$$B_{nn'} = \sum_{\nu,s}' \Psi_{\nu s}^*(n, t) \Psi_{\nu s}(n', t). \quad (6)$$

The prime attached to the summation symbol denotes the sum over states occupied by electrons in the initial state. In fact the orbital state index  $\nu$  of the time dependent electronic wave function  $\Psi_{\nu s}$  refers to the electronic eigenstate in the perfectly dimerized ground state. It is clear that, in general,  $\Psi_{\nu s}$ 's are not eigenstates of the Hamiltonian at each instance. The above equation of motion for  $y_n$  can be integrated numerically by discretizing the time variable with a step  $\Delta t$ . For the numerical simulation, we suppose a periodic boundary condition, i.e.,  $y_{N+1} = y_1$ ,  $\Psi_{\nu,s}(N+1) = \Psi_{\nu,s}(1)$ . The periodic boundary condition avoids the end point effect.

The time evolution of the electronic wave functions is calculated through the time-dependent Schrödinger equation, which can be numerically treated by the fractal decomposition method for exponential operators developed by Suzuki,<sup>21-23)</sup> choosing the time mesh  $\Delta t$  sufficiently small so that the variation of  $y_n(t)$  during  $\Delta t$  is very small in the electronic scale.

The values of parameters used in the present work are as follows;  $t_0 = 2.5$  eV,  $K = 21$  eV/Å<sup>2</sup>,  $\alpha = 4.1$  eV/Å,  $a = 1.22$  Å. These parameters correspond to a dimerization amplitude  $|y_0| = 0.078$  Å, the band gap  $2\Delta_0 (= 4\alpha|y_0|) = 1.30$  eV and the bare optical phonon energy  $\hbar\omega_Q (= \sqrt{4K/M}) = 0.16$  eV. The time mesh is set to be  $\Delta t = 0.0025 \omega_Q^{-1} (= 0.01$  fs) throughout the paper.

In the present simulation the disorder expressed by eq. (2) or eq. (3) is introduced to initiate the soliton-anti-soliton pair creation. In order to reduce the extrinsic cause as small as possible, we choose the intensity of disorder to be quite small (see the next section), although the actual value of the disorders due to dopants or bond disorders might be much larger.<sup>24-26)</sup>

### §3. Results of Simulations

In what follows, the bond variable  $y_n$  and the square amplitude of the electron wave function are express in terms of the smoothed expressions according to the following definitions,

$$\overline{y_n} = \frac{1}{4} \{ (-)^{n+1} y_{n+1} + 2(-)^n y_n + (-)^{n-1} y_{n-1} \}, \quad (7)$$

$$\overline{|\Psi_{\nu s}(n, t)|^2} = \frac{1}{4} \{ |\Psi_{\nu s}(n+1, t)|^2 + 2|\Psi_{\nu s}(n, t)|^2 + |\Psi_{\nu s}(n-1, t)|^2 \}. \quad (8)$$

### 3.1 Results for the site type disorder

In Fig. 1 we show typical examples of simulations in the form of  $\overline{y_n(t)}$ . In all the examples a single dopant with  $V_s = -0.5 \times 10^{-3}t_0$  is placed at the 60-th site. The system size is  $N = 120, 132, 144$  and  $156$  from (a) to (d), respectively. Other conditions are the same for all the cases. The common feature is a couple of initial uniform oscillations which continue up to  $t \sim 30\omega_Q^{-1}$ . The time of this initial uniform oscillation seems to depend on the strength of the dopant potential  $V_s$ . Although we did not perform any quantitative analysis, the initial oscillation time is found to get longer for a weaker potential.

After the initial uniform oscillations, the  $n$ -dependence of  $\overline{y_n(t)}$  begins to show some structures. In (b) and (c), two solitons seem to be formed and to move in opposite directions, while in (a) and (d), a bound state of the two solitons seems to be created. In the former case a localized oscillating excitation which might be regarded as a breather is left between the two solitons.<sup>11,12)</sup> It is not systematic but rather stochastic in a certain sense whether a soliton pair moving in the opposite directions is created or the created two solitons form a bound pair. By changing the system size the energy per site supplied through the electron-hole excitation is changed. A slight difference of this energy might have affected which channel of the relaxation process should be chosen.

The period of the uniform oscillation of the bond variable in the initial stage is estimated to be  $11\omega_Q^{-1}$ . Even after the formation of a soliton pair this uniform oscillation still remains, though its period become a little bit shorter ( $\sim 10\omega_Q^{-1}$ ). This period is thought to correspond to that of the renormalized optical mode, the frequency of which is known to be  $\omega_0 = 0.63\omega_Q$  ( $2\pi/\omega_0 \simeq 10\omega_Q^{-1}$ ) from the linear mode analysis for the ground state. The reason why the period of the initial uniform oscillation is slightly longer than  $2\pi/\omega_0$  is not clear. Presumably, the fact that the electron system is not in the lowest energy state would be one of possible reasons. The period of the corresponding oscillation after the formation of the soliton pair become very near to  $2\pi/\omega_0$ . This indicates that the electron system is one of the lowest energy states in the presence of the soliton type deformations. Since the soliton is a localized object, the presence of a soliton does not change the frequency of the optical mode as far as the electronic configuration is of the lowest energy.

In order to clarify the motion of the soliton pair, we show the contourgraphic presentation of  $\overline{y_n(t)}$  in Fig. 2. (a) to (d) correspond to those in Fig. 1, though the data for longer time are depicted. From this figure the speeds of the solitons in (b) and (c) are estimated to be  $2.75v_s$  and  $2.48v_s$ , respectively, where  $v_s$  ( $=\omega_Q a/2$ ) is the sound velocity of the system. In both cases the right-going and left-going solitons have different speeds. The estimated value is the average speed, of the right-

and left-going solitons. The fact that the speed of the solitons in (c) is a slightly smaller than that in (b) would be understand if we notice the initial energy supply per site is smaller in (c) than in (b).

In the case of the bound soliton pair formation, Fig. 2 (a) and (d), the relative distance between bound solitons oscillates with a frequency about  $0.63\omega_Q$  which is near the breather frequency estimated in refs. 11 and 12, although the breather like oscillation looks not very stable. It should be noted that the lattice vibrations are spreading from the bound soliton pair region.

Furthermore, in order to see the electronic structure in the case of Fig. 1 (b) (or Fig. 2 (b)), we have plotted in Fig. 3 the snapshot of the contributions to the electron density from the states,  $\psi_c$  and  $\psi_v$ , which were originally at the bottom of the conduction band and at the top of the valence band, respectively. The last one in Fig. 3 is expressed as

$$\tilde{\rho}(n, t) = \sum_{\nu, s}'' |\Psi_{\nu s}(n, t)|^2 - 1, \quad (9)$$

where the double prime on the summation symbol means the sum over all the valence band states except for the top state, the state indices representing those in the initial state. The selected time is  $t = 100\omega_Q^{-1}$ . For reference the bond variable at that time is also depicted. It will be easily understood that  $\psi_c$  and  $\psi_v$  are linear combinations of two mid-gap states located at the positions of two solitons, respectively. The holes seen in  $\tilde{\rho}$  amount to one electron for each soliton, total two electrons. The integrations of  $|\psi_c|^2$  and  $|\psi_v|^2$  yield one electron, respectively. The sum of  $|\psi_c|^2$ ,  $|\psi_v|^2$  and  $\tilde{\rho}$  is almost unity everywhere. This fact does not necessarily mean that the solitons are neutral, as will be discussed in the following.

In the present calculation, the spin of electrons is not treated explicitly except for the degeneracy. In the initial state the occupation numbers of the top of the valence band and the bottom of the conduction band are equal to unity, other valence band states being doubly occupied and other conduction band states being empty. The spin state is irrelevant since the electron-electron interactions are neglected. In this situation it will be plausible to assume the two spin states are realized with an equal probability. This means there will be no net spin density. Based on the symmetry argument Ball, Su and Schrieffer<sup>27)</sup> showed that the branching ratio of the neutral soliton pair formation versus the charged pair formation vanishes at least in the presence of the charge conjugation symmetry (or the electron-hole symmetry). This result is consistent with experiments.<sup>28,29)</sup> Even in the presence of the electron mutual interactions, namely in the absence of the charge conjugation symmetry the aforementioned branching ratio is negligibly small as argued by Kivelson and Wu.<sup>30)</sup> Although in the present work a weak disorder potential violating the charge conjugation symmetry is introduced, the result obtained in ref. 27 would be still valid.

After all these considerations, it is most natural to regard the result shown in Fig. 3 as indicating that the two branches of charged soliton pair states are realized with equal weight. Here the two

branches mean two different configurations of two charged solitons, a positive one on the left side and a negative one on the right side or vice versa. Kivelson and Wu discussed the scenario that the charged soliton pairs decay into neutral soliton pairs based on the fact that the formation energy of a neutral pair is smaller than that of a charged pair in the presence of electron mutual interactions. Since in the present treatment the electron interactions are not included, it will be plausible to assume such a decay process is not seen.

In order to see the structures of  $\psi_c$  and  $\psi_v$  more closely, we investigated the time development of  $i^n \psi_c$ ,  $(-i)^n \psi_c$ ,  $i^n \psi_v$  and  $(-i)^n \psi_v$ ; the factor  $(\pm i)^n$  is multiplied to take out the component oscillating with a wave number  $\pm k_F (= \pm \pi/2a)$ . An example of a snapshot at  $t = 100\omega_Q^{-1}$  is shown in Fig. 4 again for the case of Fig. 1(b) (or Fig. 2(b)). The smoothing procedure is applied according to eq. (8). If we express the mid-gap states related to the kinks around  $n = 30$  and  $n = 90$  by real localized wave functions  $\phi_L$  and  $\phi_R$ , respectively, the results shown in Figs. 4(a) and (b) indicate that, apart from normalization factors, the following relations are roughly satisfied,

$$\begin{aligned} \text{Re}[\overline{i^n \psi_c}] &\propto -\overline{\phi_R}, \\ \text{Im}[\overline{i^n \psi_c}] &\propto -\overline{\phi_L}, \\ \text{Re}[\overline{i^n \psi_v}] &\propto \overline{\phi_R}, \\ \text{Im}[\overline{i^n \psi_v}] &\propto -\overline{\phi_L}. \end{aligned} \quad (10)$$

which means that  $\psi_c$  and  $\psi_v$  are expressed as follows within very crude approximation,

$$\begin{aligned} \overline{\psi_c} &\propto -(-i)^n \overline{\phi_R} - i(-i)^n \overline{\phi_L}, \\ \overline{\psi_v} &\propto (-i)^n \overline{\phi_R} - i(-i)^n \overline{\phi_L}. \end{aligned} \quad (11)$$

A similar consideration based on Figs. 4(c) and (d) leads to the following relations,

$$\begin{aligned} \overline{\psi_c} &\propto i^n \overline{\phi_R} - i i^n \overline{\phi_L}, \\ \overline{\psi_v} &\propto -i^n \overline{\phi_R} - i i^n \overline{\phi_L}. \end{aligned} \quad (12)$$

Apparently different expressions eqs. (11) and (12) can be consistently satisfied if  $\psi_c$  and  $\psi_v$  (without smoothing) are expressed as

$$\begin{aligned} \psi_c &\propto -i \sin\left(\frac{n\pi}{2}\right) \phi_R(n) - i \cos\left(\frac{n\pi}{2}\right) \phi_L(n), \\ \psi_v &\propto i \sin\left(\frac{n\pi}{2}\right) \phi_R(n) - i \cos\left(\frac{n\pi}{2}\right) \phi_L(n), \end{aligned} \quad (13)$$

and the mid-gap states  $\phi_R(n)$  and  $\phi_L(n)$  are non-vanishing only at odd  $n$  and even  $n$ , respectively. Close inspection of numerical data shows that the last condition is approximately satisfied. It is a common understanding that the mid-gap state for a static soliton vanishes at every second site in the absence of electron-electron interactions. Thus it is plausible to assume the relations shown in eq. (13) to be satisfied.

The factors  $\sin(n\pi/2)$  and  $\cos(n\pi/2)$  in eq. (13) indicate that both of  $\psi_c$  and  $\psi_v$  involve  $k_F$  and  $-k_F$  components with an equal weight.  $\psi_v$  and  $\psi_c$  can be regarded also as bonding and anti-bonding combinations of two mid-gap states  $\phi_R$  and  $\phi_L$ . This fact may be most easily seen by calculating a product  $\psi_c\psi_v$  which is effectively expressed as

$$\psi_c\psi_v \propto [\phi_R(n)]^2 - [\phi_L(n)]^2 \quad (14)$$

In fact we have checked this is satisfied at least for the data shown in Fig. 4. The above results are consistent with our notion that the two different combinations of a pair of charged solitons are realized with an equal probability. This is confirmed also from the electron density profile as discussed already in connection to Fig. 3. The fact that  $\psi_v$  and  $\psi_c$  correspond to bonding and anti-bonding linear combinations of  $\phi_R$  and  $\phi_L$  can be seen from the behavior of the energy. The one-particle energy corresponding to  $\psi_v$  is slightly negative, while that corresponding to  $\psi_c$  is slightly positive, thought both of them are very near the gap center.

In order to see the behavior of the system at the initial stage of the soliton pair formation, we show in Fig. 5 snap shots (at  $t = 0, 20\omega_Q^{-1}$  and  $40\omega_Q^{-1}$ ) of the bond variable  $\overline{y_n}$  and the excess electron densities  $\tilde{\rho}_\uparrow$  and  $\tilde{\rho}_\downarrow$  for up and down spins defined by

$$\begin{aligned} \tilde{\rho}_\uparrow &= \sum_\nu'' |\Psi_{\nu\uparrow}(n, t)|^2 - \frac{1}{2}, \\ \tilde{\rho}_\downarrow &= \sum_\nu''' |\Psi_{\nu\downarrow}(n, t)|^2 - \frac{1}{2}, \end{aligned} \quad (15)$$

where  $\sum_\nu'' \dots$  means the sum over occupied up spin states and  $\sum_\nu''' \dots$  the sum over occupied down spin states. So far we did not specify the spins of the excited electron and hole. When drawing Fig. 5, we have chosen the initial occupation numbers so that there is a conduction electron and a hole in the valence band for up spin, and all the valence band states are occupied and the conduction band is empty for down spin. The electron densities have small structure even at  $t = 0$  due to the presence of the disorder potential. This small structure acts as a nucleation seed for the soliton pair formation. It should be noted that there is essentially no initial structure in the bond variable.

### 3.2 Results for the case with a bond type disorder

Here we show the results in the presence of a bond type disorder, which might mimic the mixture of a *cis*-segment in *trans*-polyacetylene. There are four different ways of putting a bond type disorder in the system. These ways correspond to four different combinations of whether the disorder is put at a single (long) bond or at a double (short) bond and whether the sign of the disorder is positive or negative.

In Fig. 6, typical results for the four different cases are depicted; the system size is fixed at  $N = 132$ . The main difference from the results for the case with the site type disorder is that the nucleation position does not necessarily coincide with the disorder position but depends on the

location and the sign of the bond type disorder. This behavior can be understood by considering whether the bond disorder is “match-type” or “mismatch-type” in the initial dimerized state.<sup>20)</sup> When the disorder is match-type, the nucleation starts at the most distant bond from the disordered one. On the other hand when the disorder is mismatch-type, the nucleation begins at the disordered bond. This will be reasonable since a bond with a match-type disorder is stable against reversing the bond variable while a bond with a mismatch-type disorder is unstable. Furthermore the free motion of solitons is not seen. This is also reasonable if we remember the bond disorder yields an effective step like potential for a soliton as discussed in ref. 20. In the present situation, solitons tend to move towards the direction where the effective potential due to the disorder increase, and this is thought to be the reason why solitons stop at a certain distance. Since the bond disorder gives a direct effect on the bond variable, the time before the formation of a soliton pair is shorter than that in the case of a site disorder with the same disorder strength.

The detailed time variation of the bond variable at the early stage is shown in Fig. 7 where  $\Delta y_n = y_n - y_1$  is used instead of  $y_n$  in order to remove the uniformly oscillating part. When the initial value of  $\overline{\Delta y_n}$  is enhanced at the disordered bond, it means that the bond disorder is match-type. On the other hand, when it is reduced, the disorder is mismatch-type. It will be clear that the soliton pair formation is triggered at the bond where the initial value of  $\overline{\Delta y_n}$  is smallest. When the disorder is mismatch-type, the inversion of the bond variable begins at the disordered bond, while, when the disorder is match-type, it starts at the most distant bond from the disordered one.

#### §4. Concluding Remarks

Starting from an electron and a hole in the uniformly dimerized background, the lattice relaxation process related to the soliton-pair formation in polyacetylene is numerically studied using the SSH model. Two kinds of local small disorders are introduced in order to trigger the soliton-pair formation; a site disorder and a bond disorder. In the case of the site disorder, the distortion of the bond variable which is necessary to create a soliton-pair begins at the disordered site irrespectively of the sign of the disorder potential. Initially the excess electronic energy is transferred to the lattice system through the electron-lattice coupling and a uniform oscillation of the bond variable continues up to  $t \sim 30\omega_Q^{-1}$  in the case with the disorder potential strength  $|V_s| = 0.5 \times 10^{-3}t_0$ . The period of this oscillation is nearly equal to that of the renormalized optical mode oscillation. The time length of the initial uniform oscillation of the bond variable increases with decreasing the potential strength  $|V_s|$ , tending to be infinite in the limit  $|V_s| \rightarrow 0$ . This initial uniform oscillation was not seen in the simulations in ref. 12, which is considered to be due to the difference in the treatment of electronic dynamics. After this uniform oscillation the bond variable begins to deform at the disordered site. Although the deformation of the bond variable suggests that two solitons have been formed, we find no local charge or spin. This is thought to be due to the fact that two different channels of a charged soliton pair formation are realized with an equal weight. This

was confirmed in terms of the behaviors of mid-gap states. Although it is not clear only from the results of present simulations whether the channels for the neutral soliton pair formation is suppressed or not, it will be reasonable to assume the suppression of those channels based on the symmetry argument by Ball, Su and Schrieffer.<sup>27)</sup> It looks rather stochastic whether the created two solitons move almost freely to the opposite directions or they form a bound pair. The bound pair state seems not very stable and is dissociated into two free solitons after some time, though it is again stochastic when it is dissociated.

In the case of a bond type disorder, the starting position of the bond order distortion changes depending on whether the bond disorder is located at the double (short) bond or at the single (long) bond and whether the sign of the disorder is positive or negative. This behavior was found to be explained by the concept of “match” and “mismatch” characteristics of the bond disorder. Since the bond disorder affects the bond variable directly, the time length of initial uniform oscillation is generally shorter for the case of a bond type disorder compared to the case with a site type disorder as far as the disorder strengths are the same order of magnitude. Within the knowledge of the present authors, there has been so far no precise analysis of the effect of bond disorders on the soliton pair formation.

In the present work, the disorder strength has been chosen to be very small in order to study intrinsic properties as far as possible. If we introduce a strong site disorder, then the trapping of one of the solitons at the disorder site can occur. Furthermore the electron-electron interactions has been neglected for the sake of simplicity. If we take into account the electron correlation, the degeneracy between the neutral and charged solitons is lifted. It will be interesting to investigate the effect of this nondegeneracy on the soliton pair formation. This will be studied in a future work.

In the real photoexcitation of a soliton pair, the non-uniformity might be created during the excitation of an electron-hole pair, e.g. due to a non-uniformity of the light intensity. In fact, if we choose a wave-packet type excitation of the electron-hole pair instead of the plane wave type excitation as treated in the present paper, the soliton pair formation becomes possible even without any disorder.<sup>31)</sup> Photoexcitation experiments using a light source intentionally made non-uniform may be interesting in this sense.

### Acknowledgments

The authors thank Dr. M. Kuwabara for useful comments. This work was partially financed by a Grant-in-Aid for Scientific Research from the Ministry of Education, Science and Culture, No. 05640446. A part of numerical calculations were performed on Facom VPP500 of Institute for Solid State Physics, University of Tokyo.

---

1) W. P. Su and J. R. Schrieffer: Proc. Natl. Acad. Sci. U.S.A. **77** (1980) 5626.

- 2) Z. Vardeny, J. Strit, D. Moses, T. -C. Chung and A. J. Heeger: Phys. Rev. Lett. **49** (1982) 1657.
- 3) L. Rothberg, T. M. Jedju, P. D. Townsend, S. Etemad and G. L. Baker: Phys. Rev. Lett. **65** (1990) 100.
- 4) W. P. Su, J. R. Schrieffer and A. J. Heeger: Phys. Rev. Lett. **42** (1979) 171, Phys. Rev. **B22** (1980) 2099.
- 5) M. J. Rice: Phys. Lett. **71A**, (1979) 152.
- 6) E. Ehrenfreund, Z. Vardeny, O. Brafman, H. Fujimoto, J. Tanaka and M. Tanaka: Synth. Met. **17** (1987) 263.
- 7) H. E. Schaffer, R. H. Friend and A. J. Heeger: Phys. Rev. **B36** (1987) 7537.
- 8) D. L. Weidman and D. B. Fitchen: *Proc. Tenth Int. Conf. Raman Spectroscopy, U. Oregon, Eugene, 1986*, pp. 12-24.
- 9) Z. Vardeny, E. Ehrenfreund, O. Brafman, H. Fujimoto, J. Tanaka and M. Tanaka: Phys. Rev. Lett. **57** (1986) 2995.
- 10) L. Rothberg, T. M. Jedju, S. Etemad and G. L. Baker: Phys. Rev. Lett. **57** (1986) 3229.
- 11) A. R. Bishop, D. K. Campbell, P. S. Lomdahl, B. Horovitz and S. R. Phillpot: Phys. Rev. Lett. **52** (1984) 671.
- 12) S. R. Phillpot, A. R. Bishop and B. Horovitz: Phys. Rev. **B40** (1988) 1839.
- 13) H. Ito and Y. Ono : J. Phys. Soc. Jpn. **54** (1985) 1194, Y. Ono and H. Ito : J. Phys. Soc. Jpn. **54** (1985) 4828.
- 14) A. Terai, Y. Ono and Y. Wada: J. Phys. Soc. Jpn. **55** (1986) 2889, *ibid* **58** (1989) 3798.
- 15) Y. Ono and A. Terai: J. Phys. Soc. Jpn. **59** (1990) 2893.
- 16) M. Kuwabara, Y. Ono and A. Terai : J. Phys. Soc. Jpn. **60** (1991) 1286.
- 17) Y. Ono, M. Kuwabara and A. Terai: J. Phys. Soc. Jpn. **60** (1991) 3120.
- 18) M. Kuwabara, Y. Ono and A. Terai : J. Phys. Soc. Jpn. **61** (1992) 2412.
- 19) S. Block and H. W. Streitwolf : J. Phys. *Condensed Matter* **8** (1996) 889.
- 20) M. Kinoshita, Y. Hirano, M. Kuwabara and Y. Ono: J. Phys. Soc. Jpn. **66**(1997) 703.
- 21) M. Suzuki: Phys. Lett. **A146** (1990) 319; *ibid* **A165** (1992) 387; J. Phys. Soc. Jpn. **61** (1992) 3015; Proc. Jpn. Acad. **69** Ser. B (1993) 161.
- 22) A. Terai and Y. Ono: Prog. Theor. Phys. Suppl. No. 113 (1993) 177.
- 23) M. Kuwabara and Y. Ono: J. Phys. Soc. Jpn. **64** (1995) 2106.
- 24) Y. Ohfuti, Y. Ono, K. Iwano, A. Terai and Y. Wada: Suppl. Prog. Theor. Phys. No. 113 (1993) 45.
- 25) K. Harigaya: Phys. Rev. **B44** (1991) 7835.
- 26) A. Yamashiro, A. Ikawa and H. Fukutome: Prog. Theor. Phys. Suppl. No. 113 (1993) 25.
- 27) R. Ball, W. P. Su and J. R. Schrieffer: J. Phys. (Paris) **44** (1983) C3-429.
- 28) J. D. Flood, E. Ehrenfreund, A. J. Heeger and A. G. MacDiarmid: Solid State Commun. **44** (1982) 1055.
- 29) J. D. Flood and A. J. Heeger: Phys. Rev. B **28** (1983) 2356.
- 30) S. Kivelson and W.-K. Wu: Phys. Rev. B **34** (1986) 5423.
- 31) H. Shimizu: a masters thesis, Toho University, February 1998.

Fig. 1. Stereographic presentation of the site and time dependence of the bond variable (smoothed as in eq. (7)); the system size  $N$  is (a) 120, (b) 132, (c) 144 and (d) 156. A single dopant with  $V_s = -0.5 \times 10^{-3}t_0$  is set at the 60-th site for all the cases. The discretized time mesh  $\Delta t$  is  $0.0025\omega_Q^{-1}$ . In (b) and (c) two solitons are excited. The excitations seen in (a) and (d) look like a bound pair of two solitons.

Fig. 2. Contourgraphic presentation of the site and time dependence of the bond variable (smoothed as in eq. (7)); the system size  $N$  is (a) 120, (b) 132, (c) 144 and (d) 156. A single dopant with  $V_s = -0.5 \times 10^{-3}t_0$  is set at the 60-th site for all the cases. The discretized time mesh  $\Delta t$  is  $0.0025\omega_Q^{-1}$ . In (b) and (c) two freely moving solitons are excited. The excitations seen in (a) and (d) are bound soliton pairs showing breather like oscillations. Light shade is upper side and dark shade is downward side.

Fig. 3. Snapshot of contributions to the excess electron density from different states for a system with the total site number  $N=132$  and the up and down spin electron numbers  $N_{e\uparrow} = 66$  and  $N_{e\downarrow} = 66$  satisfying periodic boundary condition. (a) is the bond variable. (b) and (c) are the contributions from the states initially at the bottom of the conduction band and at the top of valence band,  $\psi_c$  and  $\psi_v$ , respectively. (d) is the density of total electrons except for those two electrons. The discretized time mesh  $\Delta t$  is  $0.0025\omega_Q^{-1}$ . A disorder potential is set at the 60-th site and its intensity is  $V_s = -0.5 \times 10^{-3}t_0$ . The time is  $t = 100\omega_Q^{-1}$ .

Fig. 4. Snapshot of the smoothed wave functions. The system size  $N=132$  and the time is  $t = 100\omega_Q^{-1}$ . (a) is  $i^n\psi_c$ , (b)  $i^n\psi_v$ , (c)  $(-i)^n\psi_c$ , and (d)  $(-i)^n\psi_v$ ; the factor  $(\pm i)^n$  is multiplied to take out the component oscillating with a wave number  $\pm k_F (= \pm\pi/2a)$ . The smoothing procedure is for example,  $\overline{i^n\psi_c} = \frac{1}{4}\{i^{n-1}\psi_c(n-1) + 2i^n\psi_c(n) + i^{n+1}\psi_c(n+1)\}$  in the case of (a). Solid and broken lines represent real and imaginary parts, respectively. Intensity of the disorder potential located at the 60-th site is  $V_s = -0.5 \times 10^{-3}t_0$ .

Fig. 5. The time variation of the bond variable (the broken line, arbitrary scale) and the excess electron densities for up (the thick line) and down (the thin line) spins,  $\tilde{\rho}_\uparrow$  and  $\tilde{\rho}_\downarrow$ , in the presence of a site disorder at the 60-th site of a system with a size  $N = 132$ . The figures on the left and right hand sides show the cases with  $V_s = 0.5 \times 10^{-3} t_0$  and  $-0.5 \times 10^{-3} t_0$ , respectively. Since the excess electron densities are quite small for small  $|V_s|$ , an enhancement factor  $t_0/|V_s|$  is multiplied to them.

Fig. 6. Stereographic presentation of the  $n$  and *time* dependence of the smoothed bond variable (eq. (7)). The system size is  $N = 132$ . The bond disorder is located at the 60-st bond (=double bond) in the case of (a) and (b) as depicted in (i), and at the 61-th bond (=single bond) in the case of (c) and (d) as depicted in (ii). The bond disorder factor  $V_b$  is  $-0.5 \times 10^{-3} t_0$  for (a) and (c), and  $0.5 \times 10^{-3} t_0$  for (b) and (d). The formation of a soliton pair begins around  $t = 10\omega_Q^{-1}$ .

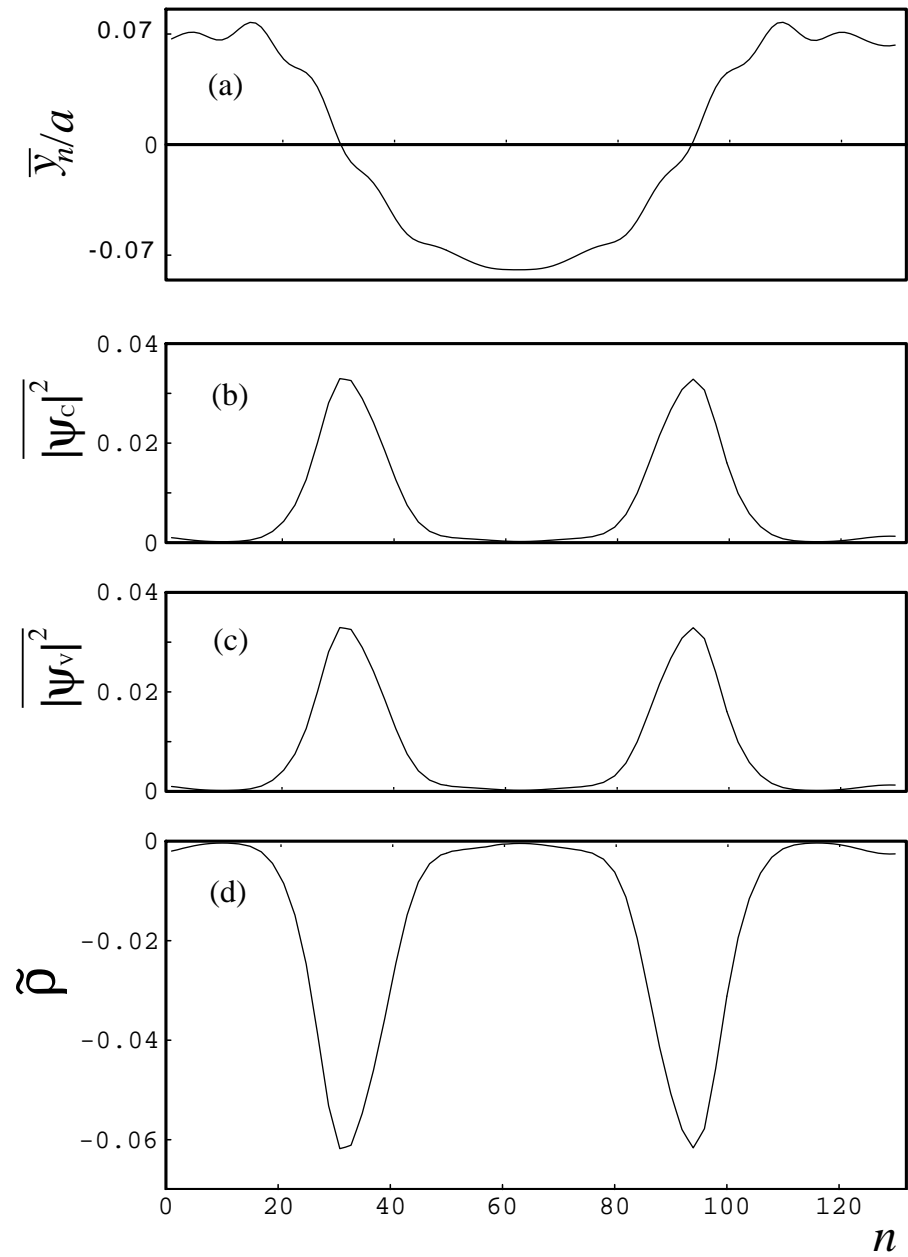
Fig. 7. The time development of the bond variable at the early stage. The system size is  $N = 132$ . Figures on the left and right hand sides show the cases with a bond disorder at the 84-th (double) and 83-rd (single) bonds, respectively. Thick lines indicate the cases with  $V_b = -0.5 \times 10^{-3} t_0$  and thin lines the case with  $V_b = 0.5 \times 10^{-3} t_0$ . The broken line shows the case without disorder for comparison. In order to remove the uniform oscillation we use  $\overline{\Delta y_n} = y_n - y_1$  instead of  $y_n$ . Since the variation of  $\overline{\Delta y_n}$  is quite small when  $|V_b|$  is small, an enhancement factor  $t_0/|V_b|$  is multiplied to  $\overline{\Delta y_n}/a$ .

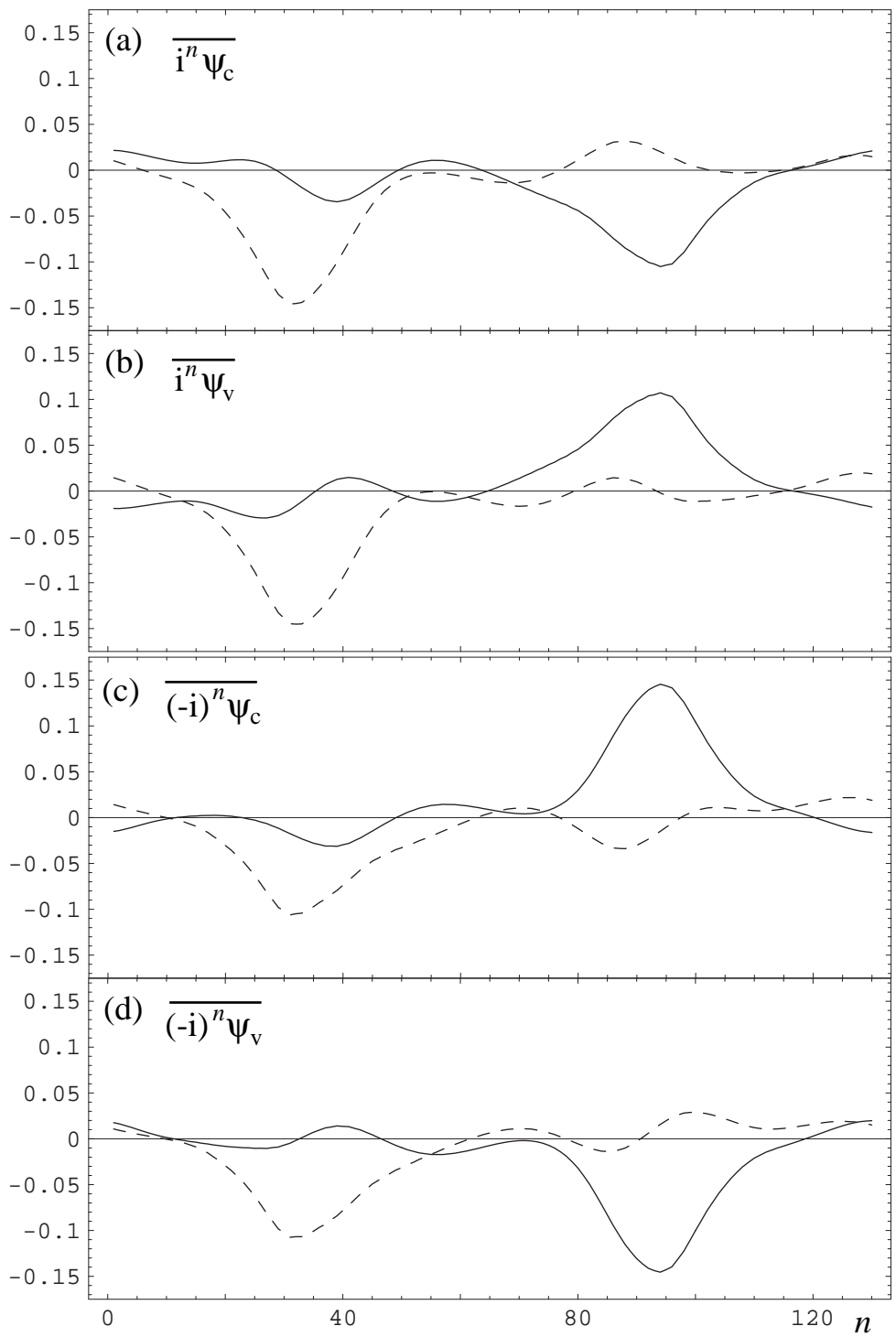
This figure "fig1.jpg" is available in "jpg" format from:

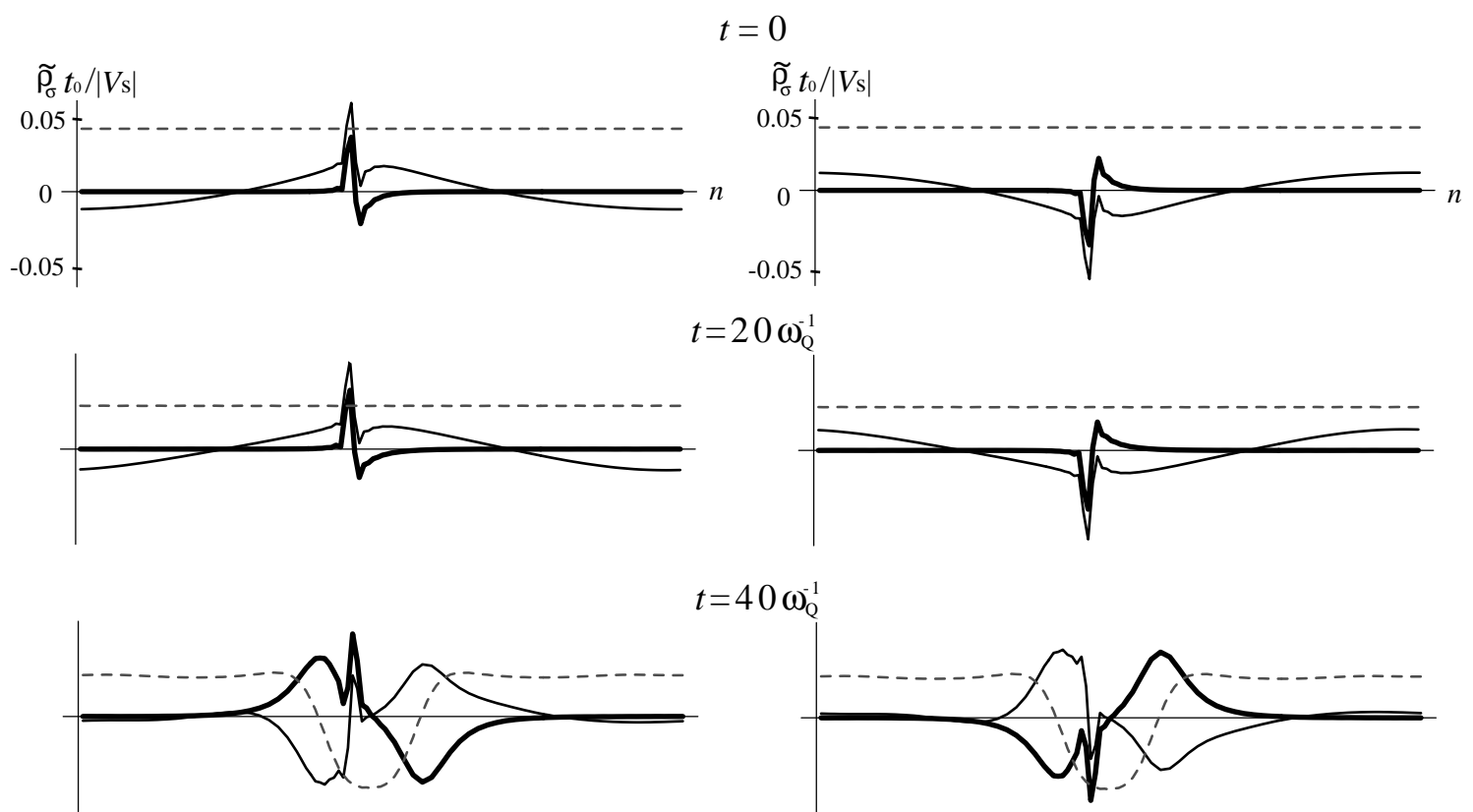
<http://arxiv.org/ps/cond-mat/9808274v1>

This figure "fig2.jpg" is available in "jpg" format from:

<http://arxiv.org/ps/cond-mat/9808274v1>







This figure "fig6.jpg" is available in "jpg" format from:

<http://arxiv.org/ps/cond-mat/9808274v1>

